Acta Universitatis Carolinae. Mathematica et Physica

Petr Kratochvíl; Pavel Lukáč; A. Svobodová

Dynamical softening of the AISI 321 steel

Acta Universitatis Carolinae. Mathematica et Physica, Vol. 31 (1990), No. 1, 47--62

Persistent URL: http://dml.cz/dmlcz/142614

Dynamical Softening of the AISI 321 Steel

P. KRATOCHVÍL, P. LUKÁČ, A. SVOBODOVÁ

Praha*)

Received 21 October 1989

The character of the hot deformation process in a wide range of deformation temperatures and strain rates was studied. The critical value of the Hollomon-Zener factor for which the dynamic recovery is replaced by dynamic recrystallization was estimated as well as the value of the activation energy of the deformation process. In both cases the dislocation substructure determines the value of the flow stress.

Byl sledován charakter deformačního procesu při deformaci za horka v závislosti na teplotě a rychlosti deformace. Určena je kritická hodnota Hollomonova-Zenerova parametru, při níž dochází k přechodu od dynamického zotavení k dynamické rekrystalizaci a také hodnota aktivační energie deformačního procesu. V obou případech dislokační struktura určuje hodnotu skluzového napětí.

Был исследован характер процесса деформации при повышенной температуре в зависимости от температуры и скорости деформации. Была определена критическая величина параметра Голломона-Зенера при которой идет переход от динамического возврата к динамической рекристаллизации и также величина активационной энергии процесса деформации. В обоих случаях дислокационная структура определяет величину напряжения скольжения.

1. Introduction

The flow stress of metallic materials is influenced by the deformation temperature T_d and strain rate $\dot{\varepsilon}$. A strong temperature dependence of the flow stress σ at low temperatures may be explained assuming that the motion of dislocations is a thermally activated process. At high temperatures $T_d > 0.4T_m$ (T_m is the melting temperature) a steady state regime, in which σ is constant, is reached in the stress – strain curve of metallic polycrystals. Both the work (strain) hardening and the softening processes take place. A steady state value of the flow stress σ_s is determined by a dynamic balance of the work hardening and softening. The softening during deformation may be associated with recovery and/or recrystallization. In such case we call them dynamic recovery (DRV) and dynamic recrystallization (DRX).

*) Department of Metal Physics, Charles University, 121 16 Praha 2, Ke Karlovu 5, Czechoslovakia.

In general, tangles or braids of dislocations may be formed during the plastic deformation. They are created due to the interaction between dislocations and they constitute obstacles to the dislocation motion causing the strain hardening. The dislocation substructure is determining σ and the ultimate strain for given deformation conditions. Simultaneously it results from the deformation process itself. A better understanding of the development of the dislocation substructure may help to identify the microphysical mechanism operating during the deformation process. It may also help to describe the macroscopical behaviour of metals deformed at higher temperatures. Any model should account not only for the influence of T_d and $\dot{\varepsilon}$, but also for hardening and softening [1].

It is a purpose of the present paper to determine the conditions under which the DRV and DRX appear in the AISI 321 steel, which is used in nuclear power stations, and to correlate the occurence of the DRV and DRX with the deformation conditions, i.e. T_d and $\dot{\varepsilon}$.

2. Phenomenological description

2.1. The flow curve

Numerous experiments show that the shape of the stress – strain curve depends on the deformation conditions. The simple shapes of the flow curves are illustrated in Fig. 1 for DRV and DRX. In the case of DRV σ increases up to the steady state value σ_s, i.e. the work hardening $\vartheta = \mathrm{d}\sigma/\mathrm{d}\varepsilon$ gradually decreases to zero. In the case of DRX the flow curve exhibits a stress maximum followed by the decrease of σ to a steady state value. At smaller $\dot{\varepsilon}$ or higher T_d the flow curve may exhibit subsidiary maxima (cyclic wave shape) as a result of the DRX followed by repeated work hardening (for a review see [1–5]).

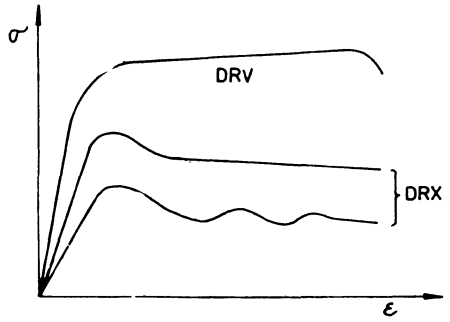

Fig. 1.

It follows from many experiments, that the strain rate and temperature dependence of σ_s during hot deformation can be described by the empirical relationship

$$Z = \dot{\varepsilon} \exp\left(Q/\mathrm{R}T_d\right) = \mathrm{A}_1[\sinh\left(\beta_1\sigma_s\right)]^n, \tag{1}$$

where Z is the so-called temperature compensated strain rate as proposed by Zener and Hollomon [6] and now generally known as the Zener-Hollomon factor, Q is the activation energy of the deformation process, R is the universal gas constant, A_1 and β_1 are material constants and the value of the "stress exponent" n is between 4 and 6 for most materials.

For practical purposes a modified eq. (1) is often used: at low stress ($\beta_1\sigma < 0{\cdot}8$) a power law

$$Z = A_2(\sigma_s/G)^n , \tag{2}$$

where G is the shear modulus and A_2 a constant; at higher stresses ($\beta_1\sigma > 1.2$) an experimental relationship

$$Z = A_3 \exp(\beta_2\sigma/G) , \tag{3}$$

where A_3 and β_2 are constants.

It should be mentioned that eqs. (1) to (3) give a good description for the strain rate dependence of σ for any strain ε and even for that at the maximum stress σ_{max} in the case of DRX [2]. Eqs. (1) to (3) are very similar to the relations describing the stress dependence of the steady state creep rate [7].

2.2. Microstructure

During DRV dislocation cells are formed in the first stage of deformation ($\vartheta > 0$). In the steady state regime ($\vartheta = 0$) subgrains are formed. They are roughly equiaxed and subboundaries are relatively narrow. Dimensions and misorientations of subgrains depend on $\dot{\varepsilon}$, T_d and on the material properties. The relationship between the mean subgrains size d_{SG} and Z is [1]

$$d_{SG}^{-1} = A_4 + A_5 \log Z , \tag{4}$$

where A_4 and A_5 are empirical constants. The dependence of d_{SG} on σ_s is very often described by [2, 8–11]

$$\sigma_s = A_6 + A_7 d_{SG}^{-n_1} , \tag{5}$$

where A_6 and A_7 are constants and n_1 lies usually in the range 1 to 1.5.

A critical strain ε_c is necessary for the onset of DRX. According to Rossard [12] ε_c is determined by

$$\varepsilon_c = 5\varepsilon_p/6 = 0.83\varepsilon_p , \tag{6}$$

where ε_p is the strain at which σ_{max} is reached. ε_c increases with decreasing T_d and increasing $\dot{\varepsilon}$, i.e. ε_c increases with increasing Z.

The dynamically recrystallized grain size d_{RX} does not change with strain during the steady state regime. d_{RX} and σ_s fulfill the phenomenological relationship [2]

$$\sigma_s = A_8 + A_9 d_{RX}^{-n_2} , \tag{7}$$

where A_8 and A_9 are empirical constants and exponent n_2 lies in the range 0.5 to 1.0 [13–17].

A criterion for the onset of *DRX* based on the driving force due to the difference in the dislocation density on the opposite sides of the grain boundary has been analyzed by Sandstron and Lagneborg [18, 19] and by Roberts and Ahlblom [20].

According to Sah et al. [17] and Roberts et al. [21] the strain dependence of the volume fraction X_R of the dynamically recrystallized material may be described by the Avrami type equation

$$X_R = 1 - \exp\left[-A_{10}(\varepsilon - \varepsilon_c)\right]^{n_3}, \tag{8}$$

where A_{10} and n_3 are constants.

3. Models based on the microstructure evolution

The motion of dislocations through the crystal is affected by many kinds of obstacles. The obstacles to dislocation motion are usually divided into two major types: (a) the large obstacles that posses the long range internal stress fields and (b) the local obstacles that posses short range stress field. When both types of obstacles are present the shear stress (and therefore the flow stress σ of polycrystals) can be considered to consist of two components, which differ from each other:

$$\tau = \tau_i + \tau_e . \tag{9}$$

where τ_i is the internal stress originating from long range stress fields (of other dislocations) and τ_e is the so called effective stress required to overcome the local obstacles. τ_i is an athermal resistance, which may be overcome by dislocations only by increasing the applied stress or by reducing the long range stress field through structural changes due to annealing processes associated with the rearrangement and annihilation of dislocations. The moving dislocations can overcome the local obstacles by thermal activation and therefore τ_e depends strongly on T_d and $\dot{\varepsilon}$.

The softening occurs at elevated temperatures and work hardening rate ϑ gradually decreases to zero, where dynamic equilibrium between strain hardening (due to the increase of dislocation density) and dislocation annihilation takes place. For high T_d the effective stress τ_e is negligibly small (it does not change with the strain ε) and therefore τ is determined by τ_i. Therefore we assume below that

(a) $\tau = \tau_i$,

(b) basic recovery mechanisms are cross slip and/or climb of dislocations

(c) a dislocation structure of a deformed crystal is determined by the total dislocation density ϱ.

During an increment of strain $d\varepsilon$ dislocations are generated and then stored (accumulated) and annihilated. A change in the dislocation density $d\varrho$ during $d\varepsilon$,

i.e. $d\varrho/d\varepsilon$ is given by the difference between an increase of ϱ due to the storage during deformation and the reduction of ϱ during the deformation due to the an nihilation. We can write

$$d\varrho/d\varepsilon = (d\varrho/d\varepsilon)_h - (d\varrho/d\varepsilon)_r . \tag{10}$$

The indices are h for hardening and r for recovery. The rate of the dislocation storage is given by

$$(d\varrho/d\varepsilon)_h = 1/bL \tag{11}$$

or

$$(\varrho/d\varepsilon)_h = K_1\varrho^{1/2}/b , \tag{12}$$

where the relation between the storage distance (mean free path, the slip distance) L and the average ϱ is

$$K_1 L = 1/\varrho^{1/2} \tag{13}$$

According to Kocks [22] the recovery is considered to be controlled by moving dislocations and

$$(d\varrho/d\varepsilon)_r = K_2 L_r \varrho/b , \tag{14}$$

where L_r is the annihilated length of dislocation per a recovery event and K_1 and K_2 are constants. The basic recovery mechanism is the cross slip. An equation of the structure evolution can be written in the form

$$d\varrho = d\varepsilon(K_1\varrho^{1/2}/b - K_2 L_r \varrho/b) . \tag{15}$$

It is well known that τ depends on ϱ according to

$$\tau = \alpha G b \varrho^{1/2} , \tag{16}$$

where α is a constant of the order of 1.

The hardening behaviour may be described by the work hardening $\theta = d\tau/d\varepsilon$. Using eqs. (15) and (16) we obtain

$$\theta = (d\tau/d\varrho)(d\varrho/d\varepsilon) = \alpha G K_1/2 - K_2 L_r \tau/2b . \tag{17}$$

It is obvious, that θ should decrease linearly with τ. Corresponding relations may be calculated for polycrystals. It is clear that eq. (17) is for polycrystals equivalent to

$$\vartheta = \vartheta_0(1 - \sigma/\sigma_0) , \tag{18}$$

where ϑ_0 is a material constant. The steady state flow stress σ_s may be experimentally obtained by the extrapolation of ϑ vs. σ plots to $\vartheta = 0$ and is

$$\sigma_s = M K_1 \alpha G b/L_r , \tag{19}$$

M is the Taylor factor.

If the climb of dislocations is the recovery mechanism, a decrease of ϱ during the strain increment $d\varepsilon$ is expressed by [23]

(20) $$(\mathrm{d}\varrho/\mathrm{d}\varepsilon)_r = K_3 D\varrho^2/\dot{\varepsilon}\,,$$

where D is the diffusion coefficient and K_3 is a constant. It is assumed, that the climb distance between the storage and the annihilation positions is proportional to the average distance between dislocations. We consider that the time necessary for a dislocation to pass the climb distance is much longer than that necessary for glide.

In the case when ϱ is reduced by both the recovery processes mentioned above, the equation determining the evolution of ϱ is

(21) $$\mathrm{d}\varrho = \mathrm{d}\varepsilon(K_1\varrho^{1/2}/b - K_2 L_r\varrho/b - K_3 D\varrho^2/\dot{\varepsilon})\,.$$

σ_s is a result of dynamic equilibrium between work hardening and dynamic recovery. According to the above discussion the steady state deformation is described by the evolution equation (21) of the dislocation substructure, which accounts for the production, storage, rearrangement and annihilation of dislocations.

4. Experimental procedure

The composition of the AISI 321 steel was (wt. %) Cr 17.58, Ni 10.46, C 0.06, Ti 0.52, Si 0.38, Mn 1.15, Fe balance. The samples of the gauge length 63 mm and diameter of 10 mm were deformed in tension. Testing machine 1186 of the fa INSTRON was used. The initial strain rate $\dot{\varepsilon}_0$ from 5.3×10^{-6} to $1.3 \times 10^{-1}\ \mathrm{s}^{-1}$ were employed at temperatures between 850 and 1200 °C (1123 – 1473 K). The mean grain size was 22 μm. The samples for both the optical and the electron microscopy were cooled after deformation by argon within 20 s to 600 °C. Below this temperature no redistribution of dislocation takes place. For the transmission electron microscopy (TEM) the usual procedure includes the spark machining to discs 3 mm in diameter, which are thinned electrolytically using double jet "Tenupol" of fa STRUERS. The electron microscope was the BS 540 of fa TESLA.

5. Results and discussion

5.1. Macroscopic observations

A serie of true stress – true strain curves showing the effect of $\dot{\varepsilon}$ and T_d is presented in Figs. 2 to 5. The effect of $\dot{\varepsilon}$ on the flow stress is shown in Fig. 2 and Fig. 3 for specimens deformed at 1273 K and 1450 K respectively. It can be seen, that the flow stress decreases with decreasing $\dot{\varepsilon}$. The influence of T_d on the shape of the flow stress curves is shown in Fig. 4 and Fig. 5 for samples deformed at an initial $\dot{\varepsilon} \equiv \dot{\varepsilon}_0 = 2{\cdot}5 \times 10^{-3}\ \mathrm{s}^{-1}$ and $\dot{\varepsilon}_0 = 5.1 \times 10^{-5}\ \mathrm{s}^{-1}$. It is obvious from Figs. 4 and 5, that the flow stress is decreasing with inrceasing T_d.

As it has been mentioned above that the θ vs. σ plot may be extrapolated to $\theta = 0$ in order to determined the steady state or so called saturation stress σ_s. In Fig. 6

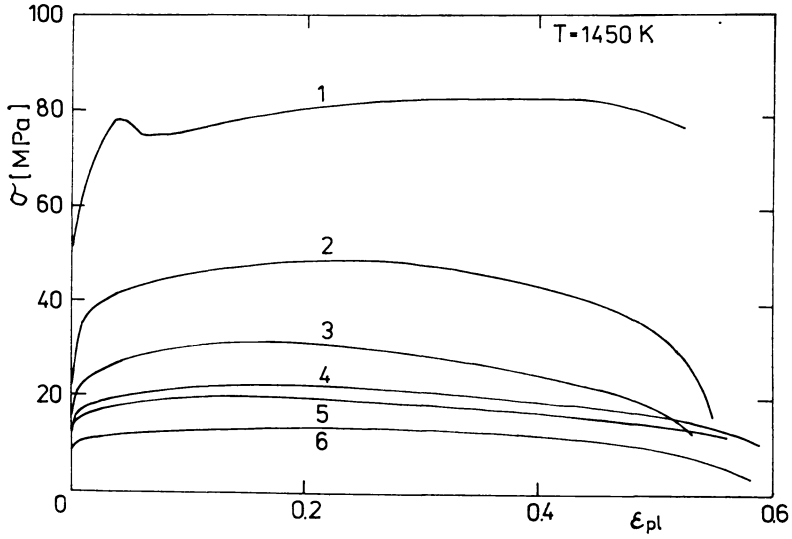

Fig. 2. Stress-strain curves at 1450 K for different strain rates:
1 — $1.3 \times 10^{-1}\ s^{-1}$ 4 — $5.1 \times 10^{-4}\ s^{-1}$
2 — $1.3 \times 10^{-2}\ s^{-1}$ 5 — $2.6 \times 10^{-4}\ s^{-1}$
3 — $2.6 \times 10^{-3}\ s^{-1}$ 6 — $5.1 \times 10^{-5}\ s^{-1}$

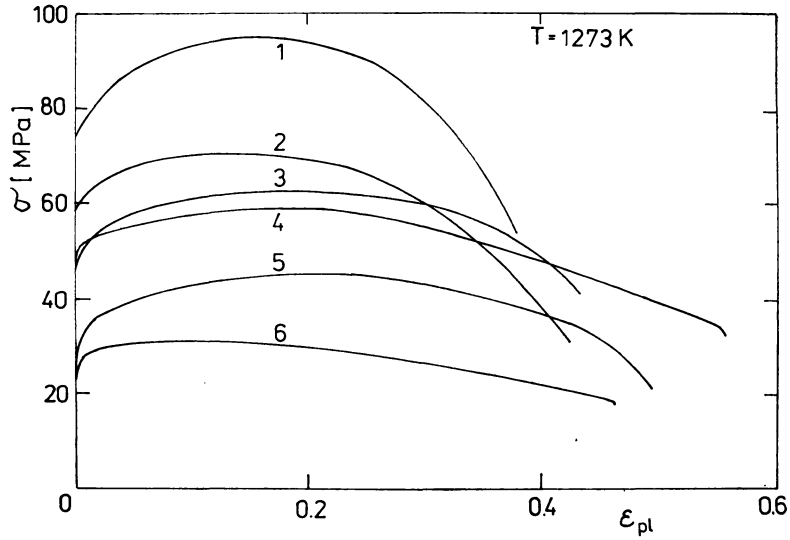

Fig. 3. Stress-strain curves at 1273 K for different strain rates:
1 — $1.3 \times 10^{-2}\ s^{-1}$ 4 — $2.6 \times 10^{-4}\ s^{-1}$
2 — $2.6 \times 10^{-3}\ s^{-1}$ 5 — $1.3 \times 10^{-4}\ s^{-1}$
3 — $5.1 \times 10^{-4}\ s^{-1}$ 6 — $2.6 \times 10^{-5}\ s^{-1}$

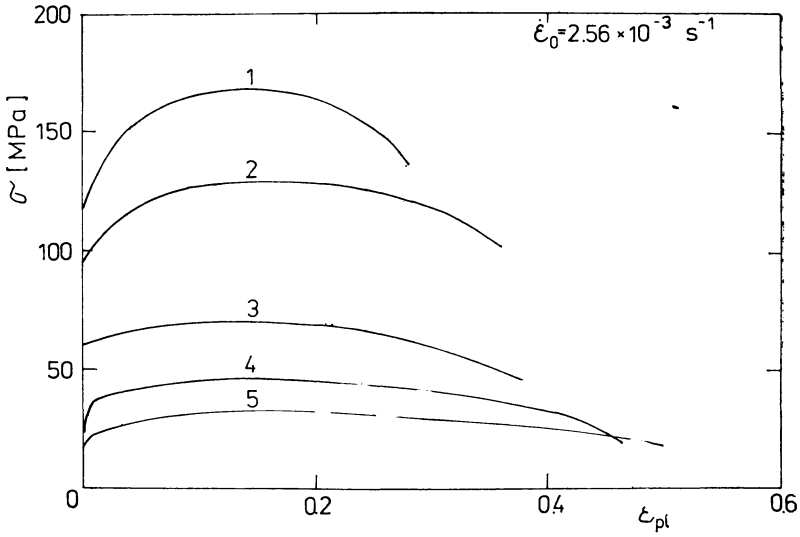

Fig. 4. Stress-strain curves with $\dot{\varepsilon}_0 = 2.6 \times 10^{-3}\ s^{-1}$ at different temperatures:
1 — 1123 K 4 — 1373 K
2 — 1173 K 5 — 1450 K
3 — 1273 K

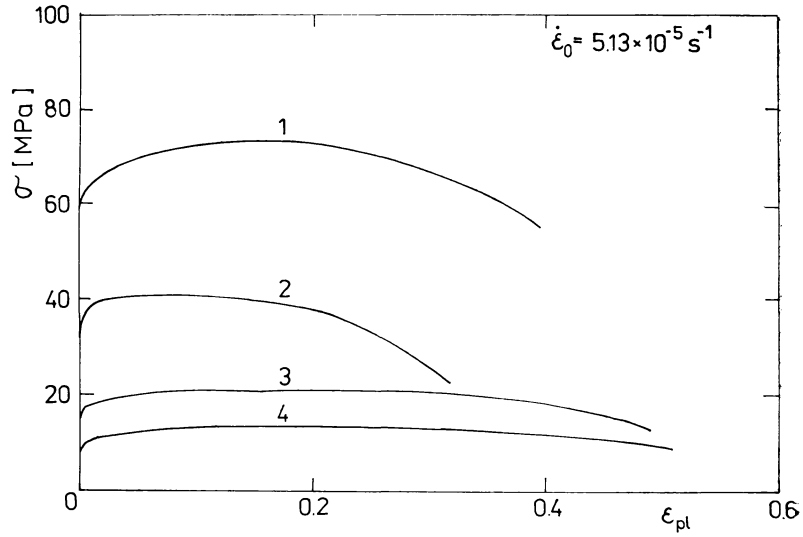

Fig. 5. Stress-strain curves with $\dot{\varepsilon}_0 = 5.1 \times 10^{-5}\ s^{-1}$ at different temperatures:
1 — 1173 K 3 — 1373 K
2 — 1273 K 4 — 1450 K

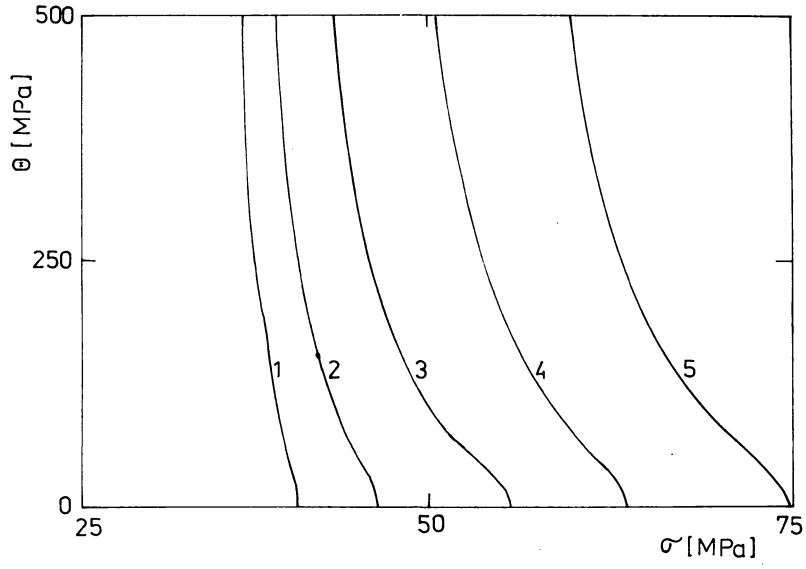

Fig. 6. σ curves at the temperature of deformation $T_d = 1273$ K for different strain rates $\dot{\varepsilon}_0$:
1 — 5.1×10^{-5} s^{-1} 4 — 5.1×10^{-4} s^{-1}
2 — 1.3×10^{-4} s^{-1} 5 — 1.3×10^{-3} s^{-1}
3 — 2.6×10^{-4} s^{-1}

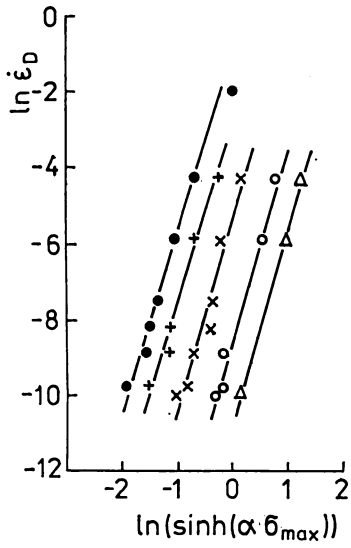

Fig. 7.

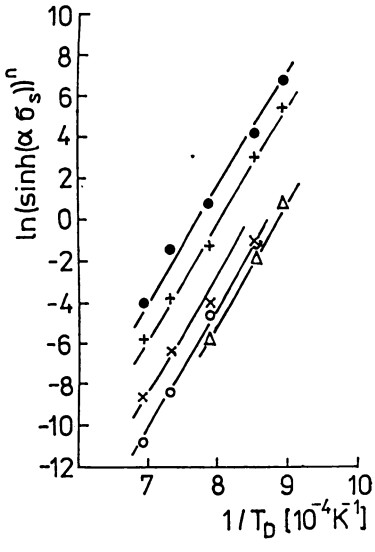

Fig. 8.

the work hardening rate θ is plotted vs. σ for samples deformed at different $\dot{\varepsilon}_0$ at $T_d = 1000$ °C. It can be seen that σ_s is increasing with increasing $\dot{\varepsilon}_0$.

In order to determine the temperature dependence of the flow stress it is important to use the values of the stress for the same internal substructure. This is very difficult at high temperatures because the softening is significant. Therefore the maximum (or the peak) stress σ_{max} is often used. According to eq. (1) $\ln [\sinh (\beta_1 \sigma_{max})]$ is plotted against $\dot{\varepsilon}_0$ in Fig. 7 for various T_d. From these plots, which should provide parallel straight lines the stress exponent n was found to be 5.5. Here we have used $\beta_1 = 1 \times 10^{-2}$ MPa^{-1}. Figure 8 shows the plots of $\ln [\sinh (\beta_1 \sigma_{max})]^n$ with $n = 5.5$ vs. $1/T_d$ for various $\dot{\varepsilon}_0$. From the average slope of these parallel straight lines the activation energy $Q = 456$ kJ/mol (4·7 eV) was determined. The values of n and Q are consistent with those obtained by Ryan and McQueen [24] for a similar AISI 317 type steel.

The simplest way how to distinguish between DRV and DRX is the criterion using the different shapes of the stress-strain curves. For all T_d starting with 1000 °C and higher DRX appears. The start of the DRX depends of course on a certain value of $\dot{\varepsilon}_0$ and of T_d. The corresponding data are given in Table I., where $\dot{\varepsilon}_c$ and Z_c for the onset of DRX are given. (For $Z < Z_c$ DRX takes place.)

Table I.

T_d (°C)	$\dot{\varepsilon}_c$(s^{-1})	Z_c(s^{-1})
1180	2.56×10^{-3}	7.0×10^{13}
1100	2.56×10^{-3}	5.8×10^{14}
1040	5.3×10^{-3}	5.7×10^{14}
1000	1.28×10^{-4}	6.8×10^{14}
950	5.3×10^{-4}	1.2×10^{15}
900	5.3×10^{-4}	8.0×10^{15}
850	5.3×10^{-5}	6.4×10^{15}

The initiation of DRX involves a critical strain ε_c. The latter can be obtained using the relation $\varepsilon_c = 0.64\varepsilon_p$ [24], which is similar to eq. (6). ε_c is given as a function of Z in Fig. 9, ε_c increases with increasing $\dot{\varepsilon}$ and decreasing T_d. This is in agreement with the general behaviour of the f.c.c. metals [13, 24–26].

5.2. Substructure

The description of the dislocation substructure complete the macroscopical observation of the true stress – true strain curves. For all cases the subgrains are typical for the hot deformation substructure. The typical substructures for differen-deformation temperatures are in Figs. 10 to 13. It is practically impossible to distint guish between the DRV and the DRX substructures as in both cases the subgrains are typical. As DRX substructure we declare that with "dislocation free" subgrains

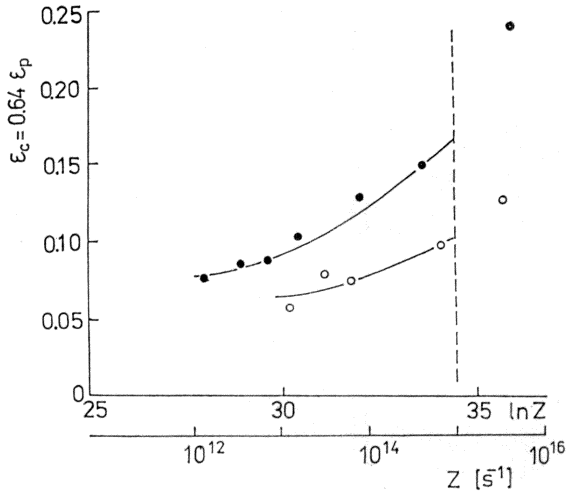

Fig. 9. The dependence of the critical strain ε_c for DRX on the value of Z.

or with the inhomogeneous distribution of dislocations with respect to the distance from the grain boundaries.

Fritzemeier et al. [27] had studied in detail the hot working and the substructure as they depend on Z. The very important statement [27] is, that the value of the flow stress σ is determined by the subgrain size d_{SG} independently on the deformation conditions (T_d and $\dot{\varepsilon}$). The relation between d_{SG} and the yield stress $0.2\,\sigma_{0.2}$ at 350 °C (Fig. 14) was determined. This plot can be described by the relation (the yield stress in MPa, the d_{SG} in μm)

$$\sigma_{0.2} = 40 + 196 d_{SG}^{-0.47} \tag{22}$$

In Fig. 14 the corresponding plot for AISI 304 steel [27] is also given. The Hall-Petch type eq. (22) has a substantially smaller exponent for the AISI 321 steel. This can be explained by a great contribution of the precipitation hardening. The total strength is often obtained with the help of the "quadratic rule":

$$\sigma = \sum_i \sigma_i^2 \tag{23}$$

The contribution σ_{SG} depending on d_{SG} is screened by the comparable value of the precipitation hardening σ_p, which does not depend on d_{SD}. Precipitation hardening in the AISI 321 type steel is due to titanium carbonitrides.

The effect of d_{SG} on σ was studied on a series of metals and alloys [2]. Any comparison is reasonable only for similar alloys as the case of AISI 321 and AISI 304 steels is. There exists also another measurement in the AISI 321 steel [28]. Here the subgrains were visualized by the replica technique extracting carbonitrides precipitated on the grain boundaries. The exponent was found to be also very near to 0.5.

Fig. 10. Dislocation substructure for $Z = 1.3 \times 10^{14}\ s^{-1}$ ($T_d = 1273$ K, $\dot{\varepsilon}_0 = 2.6 \times 10^{-5}\ s^{-1}$, $\varepsilon = 0.2$) Magn. 12 500×.

Fig. 11. Dislocation substructure for $Z = 5.8 \times 10^{13}\ s^{-1}$ ($T_D = 1373$ K, $\dot{\varepsilon}_0 = 2.6 \times 10^{-3}\ s^{-1}$, $\varepsilon = 0.2$) Magn. 39 500×.

Fig. 12. Dislocation substructure for $Z = 4.3 \times 10^{18}\ s^{-1}$ ($T_d = 1123$ K, $\dot{\varepsilon}_0 = 2.5 \times 10^{-3}\ s^{-1}$, $\varepsilon = 0.2$) Magn. 12 500×.

Fig. 13. Grain boundary dislocation after deformation at $T_d = 1373$ K. Magn. 39 600×.

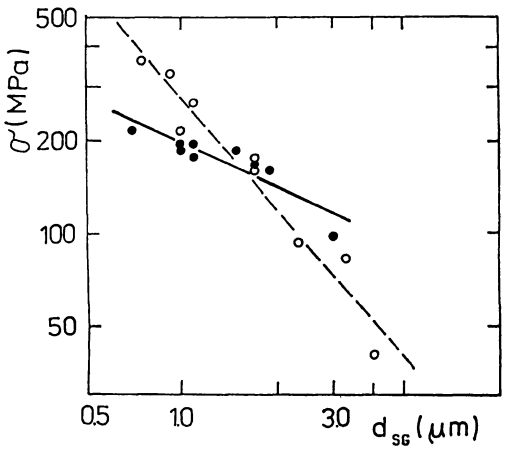

Fig. 14. The dependence of the flow stress σ on d_{SG}. The values for the AISI 304 steel (●) [27] are also given.

References

[1] McQueen, H. J., Jonas, J. J., in: Treatise on Materials Science and Technology. (ed. Arsenault R. J.). Vol. 6. Academic Press, New York 1975, p. 393.

[2] Roberts, W., in: Deformation, Processing and Structure. (ed. Krauss G.). ASM, Metals Park 1984, p. 109.

[3] Jonas, J. J., Sakai, T., ibid. p. 185.

[4] Mecking, H., Gottstein, G., in: Recrystallization of Metallic Materials. (ed. Haessner F.). Riederer Verlag, Stuttgart 1979.

[5] Sellars, C. M., Metals Forum, *4* 1981, 75.

[6] Zener, C., Hollomon, J. H., J. Appl. Phys., *15* 1944, 22.

[7] Čadek, J., Creep in Metallic Materials. Academia, Prague 1988.

[8] Jonas, J. J., Sellars, C. M., Tegart, W. J. McG., Met. Rev., *14* 1969, 1.

[9] McQueen, M. J., Wong, W. A., Jonas, J. J., Canad. J. Phys., *45* 1967, 1225.

[10] Cotner, J., Tegart, W. J. McG., J. Inst. Metals, *97* 1969, 73.

[11] Abson, D. J., Jonas, J. J., J. Nucl. Mater. *42* 1972, 73.

[12] Rossard, D. C., in: Proc. 3rd ICSMA, Vol. 2. Inst. Metals, Cambridge 1973, p. 175.

[13] Luton, M. J., Sellars, C. M., Acta Metall., *17* 1969, 1033.

[14] McQueen, J., Bergerson, S., Met. Sci., *6* 1972, 25.

[15] Glover, G., Sellars C. M., Met. Trans., *4* 1979, 765.

[16] Bromley, R., Sellars, C. M., in: Proc. 3rd ICSMA, Vol. 1, Inst. Metals, Cambridge 1973, p. 380.

[17] Sah, J. R., Richardson, G. J., Sellars, M. C., Met. Sci. J., *8* 1974, 325.

[18] Sandström, R., Lagneborg, R., Scripta Metall., *9* 1975, 59.

[19] Sandström, R., Lagneborg, R., Acta Metall., *23* 1975, 387.

[20] Roberts, W., Ahlblom, B., Acta Metall., *26* 1979, 801.

[21] Roberts, W., Boden, H., Ahlblom, B., Metal. Sci. J., *13* 1979, 195.

[22] Kocks, U. F., J. Eng. Mater. Techn. (ASME H), *98* 1976, 76.

[23] Gottstein, G., Argon, A. S., Acta Metall., *35* 1987, 1261.

[24] RYAN, N. D., MCQUEEN, H. J., Czech. J. Phys. B39 1989, 458
[25] ROSSARD, C., BLAIN, P., Mem. Sci. Rev. Met., *56* 1959, 285.
[26] PETKOVIC, R. A., LUTON, M. J., JONAS, J. J., Can. Met., Quart., *14* 1975, 137.
[27] FRITZEMEIER, L., LUTON, M. J., MCQUEEN, H. J., in: Proc. 5th ICSMA, Pergamon Press, Aachen 1979, p. 95.
[28] ELFMARK, J., Hutnické listy, 1978, 714.